



## Thermal Analysis of Salem Magnesite

D.Gopinath<sup>1\*</sup> and S. Gunasekaran<sup>1</sup>

St. Peter's Institute of Higher Education and Research, St. Peter's University, Avadi,  
Chennai-600 054, India

**Abstract :** Thermal decomposition behaviour of magnesite sample has been studied by thermogravimetric (TG) measurements. Differential thermal analysis (DTA) curve of magnesite the two endothermic peaks observed in magnesite are essentially due to de-carbonation of magnesium oxide and carbon-di-oxide respectively. The TG data of the decomposition steps have also been analysed using differential, difference-differential and integral methods, viz. **Freeman–Carroll, Horowitz–Metzger, Coats–Redfern** methods. Values of activation entropy, Arrhenius factor, and order of reaction have been compared. DSC curves for three of the magnetite samples for magnesite produced at 789, 786, and 800°C. Magnesite at 780°C a magnetite to MgO, but the sharp magnesite transition observed for magnetite formed at lower temperatures has been replaced by a very broad transition near at 789°C. It is interesting to note that the temperature for the magnesite to MgO transition decreased as the temperature for magnesite formation decreased.

**Keywords :** Magnesite, TG,DTA,DSC.

### Introduction

Magnesite is a sedimentary rock composed of more than 40% carbonate minerals. The estimated magnesite deposits in India are about 1,29,450 million tonnes [1]. magnesite, the principal raw material for steel manufacture forms one of the most important mineral deposits of India and provides a solid base for the industrial prosperity of the country. Thermal decomposition of magnesite has been the subject of intensive study over the years due to its importance in the flue gas desulfurization and in the hydration of steel in concrete. Many attempts have been made to elucidate the mechanism of the thermal decomposition of magnesite [2-10]]. Dong-Myoung Kim and Young.Woo Rhee [11] studied the sulfidation and sulfation reactions of Daesung limestone in order to investigate the reaction mechanism needed to apply new desulfurization concepts to the next generation PFBC. On the basis non-isothermal kinetic measurements, various values have been reported for the activation energy, e.g., 133–198, 101–234 kJ mol<sup>-1</sup> [12], 30.97–58.91 kcal mol<sup>-1</sup> [13], 45.14–50.80 kcal mol<sup>-1</sup> [14] and 157.79 kJ mol<sup>-1</sup> [15]. Mangaonkar et al. [16] reported the TG curves of few Indian magnesite sample. Singh and Singh [17] studied the effect of 5% tartaric, succinic and citric acids on the decomposition of magnesite carbonate and observed that the decomposition temperature was not decreased. Although the main constituent of magnesite is magnesium carbonate, certain other impurities such as calcite, silicon, aluminium, iron, alkali salts etc. are often present and they affect the decomposition reaction considerably. In view of the

D.Gopinath *et al* /International Journal of ChemTech Research, 2018,11(07): 100-106.

DOI= <http://dx.doi.org/10.20902/IJCTR.2018.110713>

importance of this phenomenon in steel materials further extension in this direction was considered necessary. The sedimentary magnesite deposits and associated rock types of the sample area belonging to cretaceous age of Indian stratigraphy.

The rock formations indicate transgressive Salem Tamil Nadu East origin. This work was undertaken in order to investigate the thermal decomposition kinetics of

Indian magnesite of Salem origin using non-isothermal thermogravimetry and differential thermal analysis. analysis was carried out to confirm the decomposition reaction at the temperature.

## 1.2 Sample preparation

Magnesium carbonate thermally decomposes to produce magnesium oxide and carbon dioxide like  $\text{MgCO}_3 + \text{heat} \rightarrow \text{MgO} + \text{CO}_2 (\text{gas})$  when heated above  $700^\circ\text{C}$  (20). Calcining at temperatures ranging from  $700^\circ\text{C}$  to  $1000^\circ\text{C}$  and its termed (LBM) light burned magnesite or caustic magnesia produces the third grades of MgO. due to the materials wide reactivity range industrial applications are quite varied and include plastics, rubber, paper and pulp processing steel boiler additives and acid neutralization to name just a few. A second type of magnesium oxide produced from calcining at temperatures ranging from  $1000^\circ\text{C}$  to  $1500^\circ\text{C}$  is termed as hard burned magnesite (HBM). Due to its narrow range of reactivity, this grade is typically used in applications where slow degradation or chemical reactivity is required such as with animal feeds and fertilizers.

Temperatures used when calcining to produce refractory grade magnesia will range from  $1500^\circ\text{C}$  to  $2000^\circ\text{C}$  and the magnesium oxide is referred as dead burned magnesite (DBM), since most if not all of the reactivity has been eliminated. Refractory grade, which is grade one magnesium oxide is used extensively in steel production to serve as both protective and replaceable linings for equipment used to handle molten steel. In the final product only MgO is present as a major compound along with few percent of CaO,  $\text{Fe}_2\text{O}_3$ ,  $\text{SiO}_2$ ,  $\text{Al}_2\text{O}_3$  as impurities.

The permissible impurities in magnesite that is to be dead burned vary depending on whether the ultimate use is to be as grain magnesite or as a constituent of magnesite brick. The effective sintering of magnesite is greatly facilitated by the presence of a few percentage of iron oxide  $\text{Fe}_2\text{O}_3$ . If the percentage of iron in the minerals is inadequate for efficient sintering, it is usually augmented by the addition of iron ore or roll scale to the crushed magnesite before calcination. the alumina  $\text{Al}_2\text{O}_3$  is interchangeable to some extent with  $\text{Fe}_2\text{O}_3$  and in maintenance grade magnesia a higher content may be allowed

### 1.2.1 Raw magnesite

The minerals for the present study have been collected from rock samples magnesite we get geographical location  $\text{N}11^\circ45.354'\text{E}78^\circ09.396'$  from TANMAG (Tamil Nadu Magnesite Limited) Salem Tamil Nadu India. The mineral rocks were crushed by hand using an agate mortar and pestle. The powdered different grade samples were subjected to analysis to get a grain size of the order of  $53\ \mu\text{m}$ . The raw sample of magnesite looking colour white

### 1.2.2 Sintering Magnesite

Magnesite up to 400mm sizes different grades was received from TANMAG (Tamil Nadu Magnesite Limited) Salem India and dumped in crusher hopper and fed to primary jaw crusher through Apron Feeder. The size was reduced to 75 mm jaw crusher. The material the size was fed to secondary crusher by belt conveyor and the size was reduced to 40mm. A Bucked elevator was used to reduce the silica 40 mm size materials is stored in kiln feed hopper and fed kiln through an automatic weight feeder and belt conveyor. The material was burnt in 9 meter long and 2.55 meter diameter rotary kiln at a specific temperature to make the required grade of magnesite. The exhaust gases were sent out through the 80 meter high chimney, the sintering materials enters 30 meter long cooler to cool down the product to  $100^\circ\text{C}$ , the sintering was done by LSHS (Long Sulphur Heavy Stock) or furnace oil (19) suppliers primary air and the secondary air was drawn through cooler. The hot zones of rotary kiln were lined with magchrome bricks and other low heat portions by alumina bricks the continuous process taken place with duration of seven hours. The raw sample of magnesite looking white and brittle undergoes changes as it is being sintering as hardens the sample undergoes colour changes from pure white to light brown

### 1.3 Experimental procedures

Thermal analysis was performed in a simultaneous TG-DTA (Netzsch STA 409) analyzer. The experimental conditions were: (a) continuous heating from room temperature to 1,000 C at a heating rate of 10 C/min; (b) N<sub>2</sub>-gas dynamic atmosphere (90 cm<sup>3</sup> min<sup>-1</sup>); (c) alumina, as reference material (d) sample: 19 mg of the sample without pressing (d) The temperature was detected with a Pt–Pt 13% Rh thermocouple fixed in a position near the sample pan. The following data was obtained by thermal analysis: (i) reaction peak temperature and main effect (endothermic or exothermic) (ii) content of bound water, which is the weight loss in the temperature range 100°C– 200 °C and content of CO<sub>2</sub> released during the decomposition of carbonate phases.

**Table 1.1 Oxide composition of magnesite samples**

Sample	MgO	SiO <sub>2</sub>	CaO	Fe <sub>2</sub> O <sub>3</sub>	Al <sub>2</sub> O <sub>3</sub>
Magnesite Grade 1	46.01	12.11	0.92	0.78	1.89
Magnesite Grade 2	45.98	12.56	0.99	0.79	1.81
Magnesite Grade 3	46.89	12.36.	0.91	0.74	1.65

### 1.4 Differential thermal analysis

The typical DTA curve of magnesite sample is presented in figure4.1. The thermal curves representing the carbonate mineral are characterized by endothermic peaks at various temperatures caused by the evolution of carbon dioxide (figure 6.1). DTA curve of magnesite shows two endotherms at 772.6°C and 834°C. The first one begins at 687°C, reaches a peak at 773°C and ends at 781°C and the second one begins at 781°C, reaches a peak at 834°C and ends at 916°C. The lower temperature peak represents the decomposition of the magnesite structure, releasing carbon dioxide from the carbonate ion associated with magnesium part of the structure accompanied by the formation of calcite and magnesium oxide.

The higher temperature peak represents the decomposition of magnesium oxide with the evolution of carbon dioxide (McInosh et al 1990). McCauley and Johnson (1999) observed the peak temperatures at 790°C and 845°C for +16 mesh dolomite samples. However, Li and Messing (1983) reported the corresponding peak temperatures for MgCl<sub>2</sub> doped dolomite sample at 750°C and 830°C. This result suggests that the presence of salt (Cl<sup>-</sup>) enhances the decomposition of magnesite the present study. The decomposition process is initiated at lower temperatures than observed for the pure magnesite. The salts promote the formation of MgO and CO<sub>2</sub> during the early stage of decomposition. The ratio of the peak area (~5.2) and the high characteristic temperature (773°C) indicates that the dolomite is in well-ordered crystalline structure (Garn 1965), which is also confirmed through X-ray diffraction analysis. According to Barcina et al (1997), smaller size of magnesium with respect to calcium facilitates the magnesium mobility and thus the formation of carbon dioxide associated to magnesium oxide is kinetically favoured against the formation of CO<sub>2</sub> associated to magnesium oxide. The first endothermic peak of dolomite, however, caused by the reaction of more complicated mechanism, has inverted symmetry/shape index of 1.45 (Garn 1965). After calcinations, the resultant oxides have lower molar volumes, larger surface areas, and greater porosities than the carbonates. The calcination of a carbonate entails the formation of an oxide having a pseudo-lattice of the carbonate and subsequent recrystallization to the normal cubic lattice of the oxide. If the temperature is high enough, sintering of oxide takes place (Glasson 1958). The results indicate that the effect of Fe<sub>2</sub>O<sub>3</sub> and Al<sub>2</sub>O<sub>3</sub> on peak temperature is maximum when these oxides are present in low concentrations.

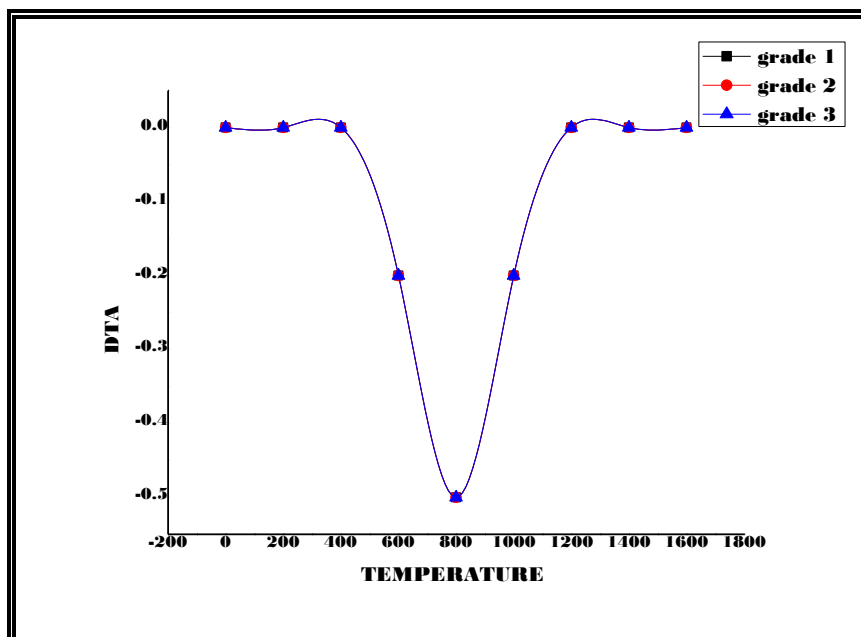


Fig 1.1 DTA of magnesite

### 1.5 Thermogravimetric analysis

The typical TG curve of dolomite sample is presented in figure 1.1. The observed weight loss was 1.33% below Table 1.1 Results of the chemical analysis of samples (%). Sample code MgO , 600°C and 850°C, it was 46.6%. The weight loss detected in the temperature range 100–120°C, was followed by a weight loss attributed to the decomposition of carbonates. The weight loss in this temperature range can be attributed to the chemically bound water. The kinetics of decomposition processes were analysed by means of the three popular methods (Freeman and Carroll 1958; Coats and Redfern 1964; Horowitz and Metzger 1963). Measured activation energies are given in table 2 and are in agreement with that reported by Criado and Ortega (1991) for pure dolomite sample.

The measured activation energy indicates that Cl- do not activate the process by lowering the thermal requirements for decomposition. The slight variation in activation energy may be attributed to the difference in particle size and mineral origin in the samples. Lower the particle size, greater the fraction of molecules located on the surface with regard to the bulk. The wide dispersion of the available data is in relation to the influence of physical processes, viz. inter- and intra-particle diffusion, heat transfer resistance, sintering etc. Garcia Calvo et al (1990) studied the influence of macro-kinetic parameters on the value of the activation energy over a wide range of experimental conditions and concluded that the influence of macrokinetic parameter is low within this range. The calculated activation energy, E, increases with increasing concentration of the decomposition product (CO<sub>2</sub>), which is similar to the observation of Ersoy-Merichoyu et al (1993). This change is attributed to the reversible nature of the decomposition reaction.

The increase in E is balanced by a corresponding increase in A which is due to the compensation behaviour. If higher activation energies are obtained, the pre-exponential factors (A) are higher too. The observed kinetic parameters were found to be strongly affected by small amounts of impurities; however, the kinetic model is not affected. Comparison of the values of E and A in the present study with those values of pure calcite reported by Garcia Calvo et al (1990) indicates that the presence of impurities is a cause of variation of kinetic parameters obtained. The impurities could function as catalysts owing to their influence in the crystalline structure. 25 0.03 0.23 0.19 46.04

**Table 2 Kinetic parameters for the thermal decomposition of the calculation Freeman–Carroll Methods**

Sample	E (kJ mol <sup>-1</sup> )	Log a (s <sup>-1</sup> )	S (JK mol <sup>-1</sup> )
Grade 1	114.56	3.89	-143.90
Grade2	114.99	3.91	-142.90
Grade3	114.76	3.76	-143.89

**Table 3 Kinetic parameters for the thermal decomposition of the calculation Coats - Redfern Methods**

Sample	E (kJ mol <sup>-1</sup> )	Log A (s <sup>-1</sup> )	S (JK mol <sup>-1</sup> )
Grade 1	114.56	3.89	-143.90
Grade 2	114.99	3.91	-142.90
Grade 3	114.76	3.76	-143.89

**Table 5 Kinetic parameters for the thermal decomposition of magnesite for the calculation Horowitz-Metzger Method**

Sample	E kJ mol <sup>-1</sup>	Log A s <sup>-1</sup>	S JK mol <sup>-1</sup>
Grade 1	114.56	3.89	-143.90
Grade2	114.99	3.91	-142.90
Grade3	114.76	3.76	-143.89

### 1.6 Differential Scanning Calorimetry

Magnesite particles was conducted in two stages. First, raw magnesite was heated for 30 hours at 650°C and then cooled very slowly. After cooling, the material was gently crushed to form a fine powder. In the second stage of magnesite approximately 200 mg of this material was placed in a Pt crucible and hung in the hot zone of a controlled atmosphere gas mixing furnace. The gas mixture was set to a reducing condition of 95% CO<sub>2</sub> and 5% CO. Higher concentrations of CO in the mixture at the temperature range of these experiments would result in the precipitation of carbon in the sample [3].

Samples were slowly heated (50°C/hr) in the gas mixing furnace to a set point temperature (i.e., 300, 450, 550, 650, 750, and 800°C), where the temperature was held for 1 hour and then cooled to ambient temperature. The actual temperature of the hot zone that the sample experienced in the gas mixing furnace was approximately 25°C below the set points. Thermal and mineralogical properties of Magnesites were characterized by differential scanning calorimetry (DSC). In order to oxidize magnesite during DSC runs, samples were heated in a pure O<sub>2</sub> carrier gas at atmospheric pressure (1 bar).

Formation temperature has a substantial effect on the thermal stability and particle size of magnetite. DSC curves for three of the synthetic magnetite samples are shown in Figure 1.2 for magnesite produced at 789, 786, and 800°C. The first broad exothermic transition in each curve at ~750°C, ~780°C, and ~800°C for magnesite produced at 789, 786 and 800°C, respectively, is attributed to the magnesite to MgO transition. The second much sharper exothermic transition represents the oxidation of MgO.

The mineralogy of these phases after each transition was verified by XRD analysis (i.e., in separate experiments, runs were stopped after a transition and the product was characterized by XRD). Magnesite at 780°C had a magnetite to MgO, but the sharp magnesite transition observed for magnetite formed at lower temperatures has been replaced by a very broad transition near at 789°C. It is interesting to note that the temperature for the magnesite to MgO transition decreased as the temperature for magnesite formation decreased.

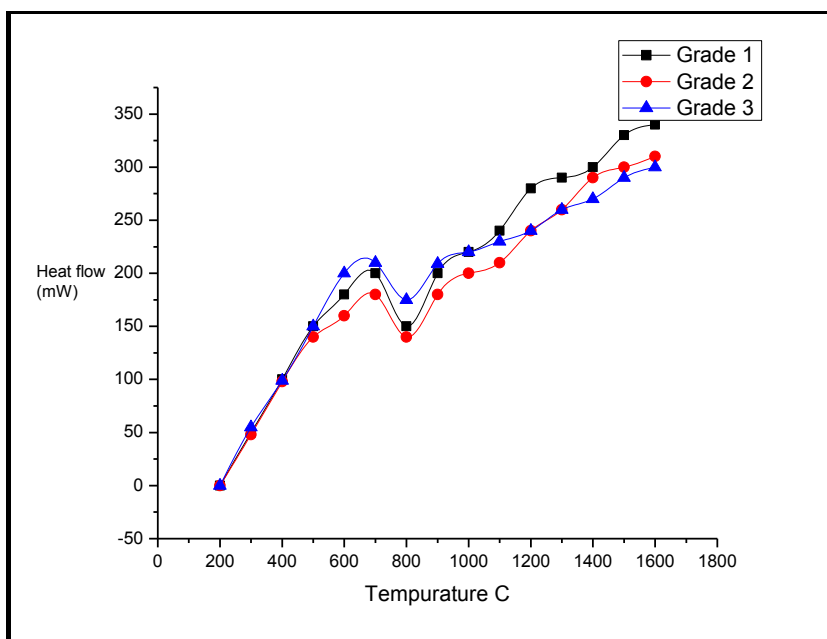


**Fig 1.2 . DSC heat flow curves for three magnetite samples formed at 789, 786, and 800°C (numbers represent temperature set points in gas mixing furnace, but temperatures in the furnace hot zone was 25°C lower).**

## Conclusions

DTA curve of Magnesite shows two peaks at 777.8°C and 834°C. The two-stage decomposition reaction is confirmed. At 750°C, the Magnesite structure is changed into MgO, which is confirmed by the thermal decomposition reaction. The large fluctuation in the observed activation energies is due to the presence of impurities in the samples. The impurities could function as catalysts owing to their influence in the crystalline structure. The results show that the clay with which they are heated which is reflected by the differences in the activation energy, affects Magnesite decomposition. These results could be important in site consideration of the Magnesite sample. DSC curves for three of the magnetite samples are shown in Figure 6.2 for magnesite produced at 789, 786, and 800°C. Magnesite at 780°C had a magnetite to MgO, but the sharp magnesite transition observed for magnetite formed at lower temperatures has been replaced by a very broad transition near at 789°C. It is interesting to note that the temperature for the magnesite to MgO transition decreased as the temperature for magnesite formation decreased.

## References

1. Zhao, YN, Zhu, GZ. Thermal decomposition kinetics and mechanism of magnesium bicarbonate aqueous solution. *Hydrometallurgy*. 2007;89:217–223. 10.1016/j.hydromet.2007.07.006.
2. Özdemir, M, Çakır, D, Kıpçak, İ. Magnesium recovery from magnesite tailings by acid leaching and production of magnesium chloride hexahydrate from leaching solution by evaporation. *Int J Miner Process*. 2009;1:209–212. 10.1016/j.minpro.2009.08.001.
3. Demir, F, Dönmez, B. Optimization of the dissolution of magnesite in citric acid solutions. *Int J Miner Process*. 2008;1:60–64. 10.1016/j.minpro.2008.01.006.
4. Wang, HM. Status and development trend of China's magnesite. *China Non-Metal Min Indus Her*. 2007;6:57–60.
5. Bertol, CD, Cruz, AP, Stulzer, HK, Murakami, FS, Silva, MAS. Thermal decomposition kinetics and compatibility studies of primaquine under isothermal and non-isothermal conditions. *J Therm Anal Calorim*. 2010;102:187–192. 10.1007/s10973-009-0540-3.
6. Liu, P, Thomas, PS, Ray, AS, Guerbois, JP. A TG analysis of the effect of calcination conditions on the properties of reactive magnesia. *J Therm Anal Calorim*. 2007;88:187–192.
7. L'vov, BV. 2002 Mechanism and kinetics of thermal decomposition of carbonates. *ThermochimActa*. 386:1–16. 10.1016/S0040-6031(01)00757-2.

8. Lu, RY, Dong, J. Kinetics of thermal decomposition of magnesite in nitrogen. *J Guizhou Univ Nat Sci.* 2009;2:45–47.
9. Vyazovkin, S, Sbirrazzuoli, N. 2006 Isoconversional kinetic analysis of thermally stimulated processes in polymers. *Macromol Rapid Commun.* 27:1515–1532. 10.1002/marc.200600404.
10. Peterson, JD, Vyazovkin, S, Wight, CA. Kinetics of the thermal and thermooxidative degradation of polystyrene, polyethylene and polypropylene. *Macromol Chem Phys.* 2001;202:775–784. 10.1002/1521-3935(20010301)202:6<775::AID-MACP775>3.0.CO;2-G.
11. Niu, SI, Han, KH, Lu, CM, Sun, RY. Thermogravimetric analysis of the relationship among calcium magnesium acetate, calcium acetate and magnesium acetate. *Appl Energy.* 2010;87:2237–2242. 10.1016/j.apenergy.2010.01.007.
12. Al-othman, AA, Al-Farhan, K, Mahfouz Refaat, M. 2009 Kinetics analysis of nonisothermal decomposition of  $(\text{Mg}_5(\text{CO}_3)_4(\text{OH})_2 \cdot 4\text{H}_2\text{O}/5\text{Cr}_2\text{O}_3)$  crystalline mixture. *J King Saud Univ Sci.* 21:133–143. 10.1016/j.jksus.2009.04.001.
13. Friedman, HL. Kinetics of thermal degradation of char-forming plastics from thermogravimetry. Application to phenolic plastic. *J Polym Sci C Polym Symp.* 1964;6PC:285–292.
14. Li, XY, Wu, YQ, Gu, DH, Gan, FX. 2009 Thermal decomposition kinetics of nickel(II) and cobalt(II) azobarbituric acid complexes. *Thermochim Acta.* 493:85–89. 10.1016/j.tca.2009.04.010.
15. Zheng, HX, Liao, XS, Wang, Q, J, Li. TG kinetics of decomposition of magnesite powder and its pellet. *J Univ Sci Technol Liaoning.* 2008;31:29–31.
16. Kissinger, HE. Reaction kinetics in different thermal analysis. *Anal Chem.* 1957;29:1702 10.1021/ac60131a045.
17. Hu, RZ, Shi, QZ. Thermal analysis kinetics. Beijing: Science Press; 2001.
18. Samtain, M, Dollimore, D, Alexander, KS. 2002 Comparison of dolomite decomposition kinetics with related carbonates and the effect of procedural variables on its kinetics parameters. *Thermochim Acta.* 392–393:135–145. 10.1016/S0040-6031(02)00094-1.
19. Ning, ZQ, Zhai, YC, Sun, LQ. 2009 Study on the thermal decomposition kinetics of magnesium hydroxide. *J Mol Sci.* 25:27–30.
20. Zheng, Y, Chen, XH, Zhou, YB, Zheng, C. The decomposition mechanism of  $\text{CaCO}_3$  and its kinetics parameters. *J Huazhong Univ Sci Technol.* 2002;12:86–88.
21. Wang, SJ, Lu, JD, Zhou, H, Hu, ZJ, Zhang, BT. 2003 Kinetics model study on thermal decomposition of limestone particles. *J Eng Thermophys.* 24:699–702.

\*\*\*\*\*